Available online at www.sciencedirect.com
ScienceDirect
Journal of Power Sources 176 (2008) 547–554
JOURNAL OF POWER SOURCES
www.elsevier.com/locate/jpowsour

Progress in high-power nickel–metal hydride batteries

Peter Bäuerlein *, Christina Antonius, Jens Löffler, Jörg Kümpers

VARTA Automotive Systems GmbH, Am Leineufer 51, D-30419 Hannover, Germany

Available online 25 August 2007

Abstract

High demands to power performance, high cycle and calendar life as well can be met by NiMH batteries, making this battery system very suitable for HEV applications. The hydrogen storage alloy plays an important role with respect to power performance and life duration. Power performance and cycle life behaviour are related to each other by the electrochemical and mechanical properties of the alloy, via a more or less reciprocal relationship. In terms of power performance at medium-discharge rates, the charge transfer reaction at the hydrogen storage alloy interface was found to be crucial for the temperature-dependent behaviour of the cell, whereas at discharge rates above about 15*C* diffusion limitation was found especially at the negative electrode. The alloy corrosion is taking place in alkaline media, leading to the formation of surface films and a change of the chemical composition, especially in near surface regions of the alloy particles. Consecutive electrochemical cycles lead to mechanical stress and finally cracking of the alloy particles. Stability against corrosion and pulverisation on one hand and good electrochemical performance on the other hand both depend on the chemical composition of the alloy, its morphological properties and the cycling regime used.

Keywords: Nickel–metal hydride batteries; Hydrogen storage alloy; Power performance of NiMH batteries; Cycle life of NiMH batteries

1. Introduction

Alkaline batteries have been playing an important role in the field of electric energy storing devices for more than 100 years. Since the discovery of the nickel–iron accumulator by Edison and of the nickel–cadmium battery system by Jungner [1,2] a multitude of inventions has contributed to make alkaline rechargeable electrochemical energy storing systems viable for a big market.

By end of the 1980s of the last century the nickel–metal hydride system appeared on the market [3,4]. Main change to the other nickel-based rechargeable systems is the replacement of the anode by a material capable of reversibly storing hydrogen. This development was enabled by the availability of new hydrogen storing alloys which are stable under exposure to strong caustic media and a high number of charge/discharge cycles [5,6]. Increased specific capacities and high-capacity densities of the negative electrode resulting from the employment of these hydride materials have been the reason for a considerable increase of energy storing capacity of cells manufactured therewith. NiMH batteries have continuously taken over the biggest part of the earlier NiCd market since that time. The main advantage of alkaline batteries in vehicles is their high charge and discharge power capability and their good long-term endurance. Despite of the higher price in comparison to lead-based batteries, NiMH battery systems have therefore been mainly used for those applications where lead acid batteries exhibited weak behaviour, which are high-continuous discharge power capability, fast recharge and long-service life, particularly in terms of capacity turnover. Because of these properties the NiMH battery system is very suitable for hybrid electric vehicle (HEV) applications.

2. Experimental

The power performance was studied in different conventional cell types but also in a special setup comprising a conventional jelly roll and a Hg/HgO reference electrode. However, the differences in electrical connection of the jelly roll to the current collector resulted in a higher ohmic resistance for the reference electrode setup, reported resistance values were therefore corrected by the setup immanent resistance of 0.9 mΩ.

For cycle life measurements AA-size cells were used. The negative electrode consisted of a mixture of 97% of alloy and 3% of conductive binder. The positive electrode was a pasted

* Corresponding author at: VARTA Automotive Systems GmbH, B.U. Advanced Systems, Am Leineufer 51, 30419 Hannover, Germany.
Tel.: +49 511 975 1835; fax: +49 511 975 1805.
E-mail address: peter.baeuerlein@jci.com (P. Bäuerlein).

0378-7753/$ – see front matter © 2007 Elsevier B.V. All rights reserved.
doi:10.1016/j.jpowsour.2007.08.052

electrode using nickel foam as a substrate. A PP/PE separator was used in combination with 7N alkaline electrolyte. The cells were cycled under different cycling regimes at various temperatures and characterised by pulse power tests [7] or high-rate discharge frequently.

After cycling and electrochemical characterisation, the cells were discharged to 0.9 V prior to dismantling. The jelly roll was transferred into test cell container flooded with alkaline electrolyte. A nickel foam counter electrode was used to charge and discharge positive and negative electrode independently from each other, Hg/HgO was used as a reference electrode. The negative charge excess capacity, the capacity of negative and positive electrodes, respectively, were determined. For chemical and physical analysis positive and negative electrodes removed from a cycled cell were rinsed with water several times before drying. The chemical composition of each electrode was determined by an inductively coupled argon plasma emission spectrophotometer. For the characterisation of the alloy particle decrepitation behaviour and of the structure of the interface layer, the negative electrode was examined by means of scanning electron microscopy (SEM) and transmission electron microscopy (TEM).

3. Results and discussion

3.1. Power performance of NiMH cells

Power performance is a key issue for the use of battery systems in high-power applications as hybrid electric vehicles. In the case of NiMH batteries special interest was focussed on the influence of the chemical composition [8–13] of the hydrogen storage alloy or special activation procedures to increase power performance [14–16] up to now. On the other hand a great number of publications can be found dealing with fundamental electrochemical studies of the hydrogen evolution reaction (HER) at various electrodes [17–19]. Iwakura et al. [20,21] studied the electrochemical reactions taking place at the surface of hydrogen storing alloys during the charge reaction in detail. The initial step for the evolution of hydrogen but also for the hydrogenation of battery alloy material is splitting of water and the adsorption of a hydrogen atom at the surface of the electrode material according to Eq. (1), this charge transfer reaction is well known as the Volmer reaction.

$$M + H_2O + e^- \rightarrow \{MH\}_{ads} + OH^- \quad (1)$$

The adsorbed hydrogen phase can react in different ways. The preferred reaction in terms of charging of NiMH cells is the formation of the hydride phase according to (2). However, if the hydrogen diffusion into the bulk alloy is much slower compared to the charge transfer step, hydrogen gas can be produced via the Tafel reaction (3) and the Heyrovsky reaction (4) as well:

$$\{MH\}_{ads} \rightarrow \{MH\}_{hydride} \quad (2)$$

$$2\{MH\}_{ads} \rightarrow 2M + H_2 \quad (3)$$

$$\{MH\}_{ads} + H_2O + e^- \rightarrow M + H_2 + OH^- \quad (4)$$

A more detailed reaction scheme has to consider mass transport phenomena and chemical reactions as well. The formation of the hydride phase first occurs at the surface of the hydrogen storage alloy. For complete hydrogenation, hydrogen has to be transported from the surface to the bulk of the alloy. As water molecules are taking part in the charge transfer reaction by playing the role of a proton donor, water must be transported to the double layer via diffusion. Hydroxide ions as the reaction product have to be removed from the double layer to the electrolyte bulk. Similar reactions can be formulated for the positive electrode as well. Each of the reactions described, may be rate determining during charge and discharge of a NiMH cell depending on the cycling conditions used.

In order to get more information about the mechanisms taking place during the discharge process of a NiMH cell, especially at low temperatures, pulse tests were performed at different temperatures. A 5*C* pulse current was chosen, in order to prevent effects caused by mass transport limitations especially at lower temperatures. Potentials of the positive and negative electrode, respectively, can be measured independently by means of a Hg/HgO reference electrode during operation in a experimental setup. The resistance measured at short-pulse periods, therefore including the electronic resistance in the electrodes, the bulk resistance of the electrolyte, and also the charge transfer resistance, needs to be corrected by the setup immanent resistance of about 0.9 mΩ. Fig. 1 shows the temperature dependence of the resistance of the positive electrode and of the negative electrode during a 25 s current pulse at a 5*C* rate. Both electrodes show an increasing pulse resistance with decreasing temperature. However, the temperature dependency of the resistance of the negative electrode is much more pronounced compared to the positive electrode. In addition a steeper increase was found to occur between +10 and 0 °C at the negative electrode, which was not observed at the positive electrode. Under these pulse conditions, the negative electrode is the main contributor to the cell resistance and power performance of the NiMH cell at low temperatures. In addition, high-rate pulses were performed, indicating severe mass transport limitations at the negative electrode at low temperatures around 0 °C and at high-pulse currents with more than 15*C* rate.

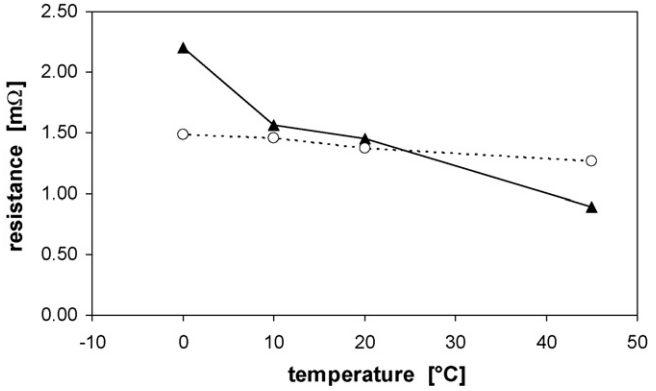

Fig. 1. 25 s/5*C* pulse resistances for the negative and the positive electrode in a test setup comprising of a NiMH jelly roll of 10 Ah capacity cell and a Hg/HgO reference electrode as a function of temperature ((◯) positive electrode; (▲) negative electrode).

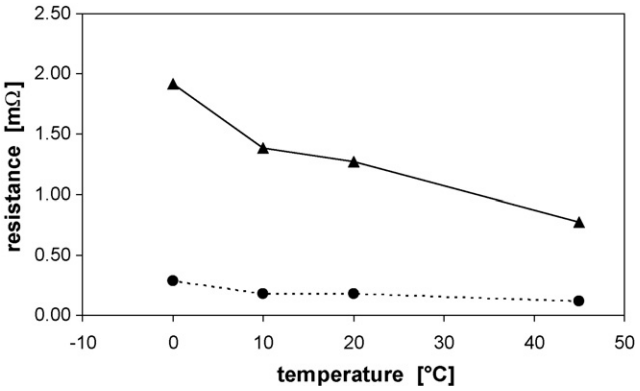

Fig. 2. 5*C* pulse resistances for the negative electrode in a test setup consisting of a 10 Ah NiMH jelly roll and a Hg/HgO reference electrode as a function of temperature ((▲) 1 s resistance negative electrode; (●) 25 − 1 s resistance negative electrode).

The total electrical resistance determined during a 25 s pulse may be split up with respect to pulse time. The short-time part (at around 1 s or below) contains the electronic resistance of electrodes, substrates, current connectors, the bulk electrolyte resistance and the charge transfer resistance as well. The medium-time part (between 1 and 25 s) is mainly caused by diffusion (see Fig. 2). The total resistance of the negative electrode is dominated by the short-time resistance. It decreases from 1.9 mΩ at 0 °C to about 0.8 mΩ at 45 °C. From all resistance parts contributing to the short-time resistance, the bulk electrolyte resistance and the charge transfer resistance are expected to dominate the temperature dependency. Since the contribution of the bulk electrolyte resistance to the pulse resistance of a NiMH cell is rather small, the charge transfer resistance is expected to have the main contribution to the short-time resistance. It is also expected to be the most obvious for the explanation of the temperature dependency, whereas the changes in the diffusion related resistance are small compared to the former. These results are in good accordance with the existing literature, indicating that the discharge reaction in NiMH cells at low temperature is controlled by the charge transfer process at the solid/electrolyte interface of the negative electrode [8,22,23].

As the charge transfer reaction is expected to take place at the alloy–electrolyte-interface, TEM was used to study the interface layer of hydrogen storage alloys exposed to alkaline electrolyte. Fig. 3 shows a TEM image of a hydrogen storage alloy harvested from a NiMH cell after a few charge discharge cycles. The surface of the alloy material was covered with needle shaped deposits, which consist of rare earth hydroxides. Between these surface deposits and the bulk alloy, two interface layers with thicknesses of 120 and 30 nm were observed. The interface layers showed a polycrystalline structure and comprise alloy elements as confirmed by energy dispersive X-ray analysis (EDX). However, oxygen was found to be also present in these interface layers. Oxygen was preferably located at the surface layer exposed to alkaline electrolyte, La^{3+} was found to be present in this area too.

The needle-like deposits of rare earth hydroxides and the polycrystalline interface layers covering the bulk alloy are both

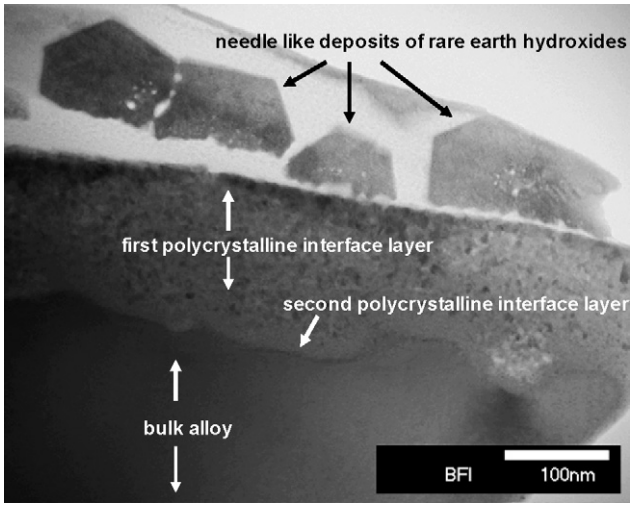

Fig. 3. TEM of an hydrogen storage alloy harvested from a NiMH cell exposed to only a few number of electrochemical cycles.

generated by corrosion processes of the alloy in strong alkaline media. The interface layers in principle may contribute to an increase of the resistance of the negative electrode. Composition, structure and thickness of these interface layers may therefore play an important role with respect to charge transfer rate, hydrogen evolution reaction or hydrogen diffusion rates, as they may possibly react as a barrier. The effect of interface layers with respect to power performance and the growth of these layers as an effect of aging has been pretty well studied by many authors at the Li-ion battery system [24,25]. Especially, in the case of nickelate-based cathodes, the formation of an interface layer at the cathode active material has been the main reason for power fade during cell aging [26,27].

As soon as AB_5-type hydrogen storage alloys are exposed to alkaline electrolytes, corrosion reactions are taking place, starting at the surface of the alloy. Both, the extent of corrosion and the corrosion rate, depend on the chemical composition of the alloy to a high degree. The thermodynamic stability of the hydride phase is also related to the chemical composition of

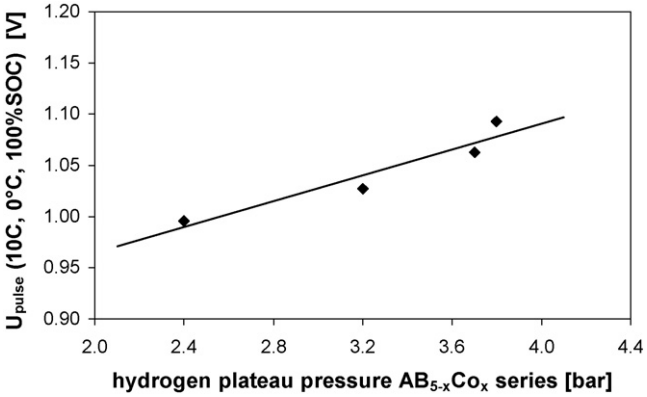

Fig. 4. Relationship between hydrogen plateau pressure of hydrogen storage alloys and power performance of NiMH cells manufactured with these alloys. Discharge was performed on fully charged cells at 10*C* rate and a temperature of 0 °C, voltage was plotted after 0.15 Ah of discharged capacity to prevent misleading effects coming from cell warming during discharge.

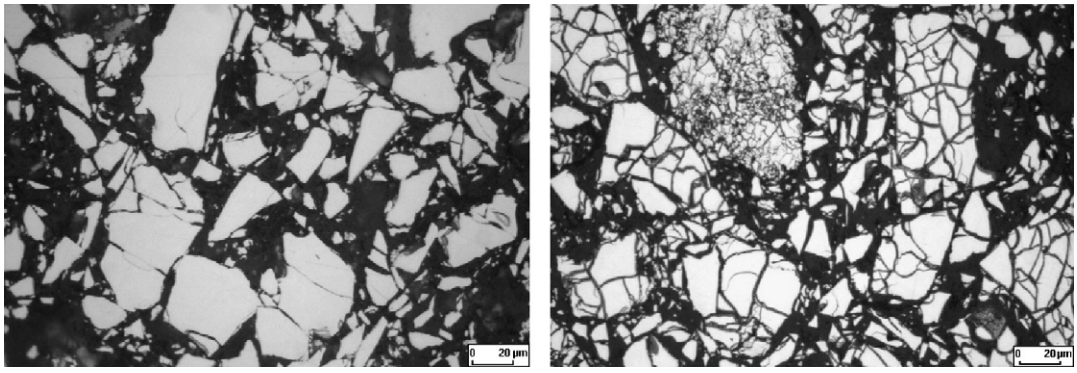

Fig. 5. SEM of fresh alloy and alloy removed from a NiMH cell, exposed to electrochemical cycles.

AB_5-type hydrogen storing alloy, as the hydrogen pressure in the plateau region is directly correlated to the M–H interaction energy. In addition, the rates of reactions (1)–(4) are determined by the M–H interaction energy [12,28]. Hydrogen de-intercalation from the hydride phase becomes faster as the M–H interaction energy decreases. Consequently, alloys showing a high-plateau pressure should provide better power performance compared to alloys forming a more stable hydride phase. For a series of AB_5-type alloys according to $AB_{5-x}Co_x$ with variation of Co content, the plateau pressure decreases with increasing cobalt content. Consequently, the rate capability, characterised by the voltage recorded after discharge of 0.15 Ah from fully charged cells at 0 °C and 10*C* rate, decreases (see Fig. 4).

However, even in this series with minor changes in the chemical composition of the alloy, the variation of the hydrogen plateau pressure is not the only property, which changes with composition. Hydrogen intercalation into the AB_5 host lattice is accompanied by an increase of the unit cell volume. This increase depends on the chemical composition of the alloy and the content of intercalated hydrogen. Consecutive lattice expansion and contraction during hydrogen intercalation and extraction produces mechanical stress, finally leading to the cracking of alloy grains. As a result the particle size of the alloy is reduced and the surface area of the negative electrode increases with consecutive electrochemical cycling (see Fig. 5).

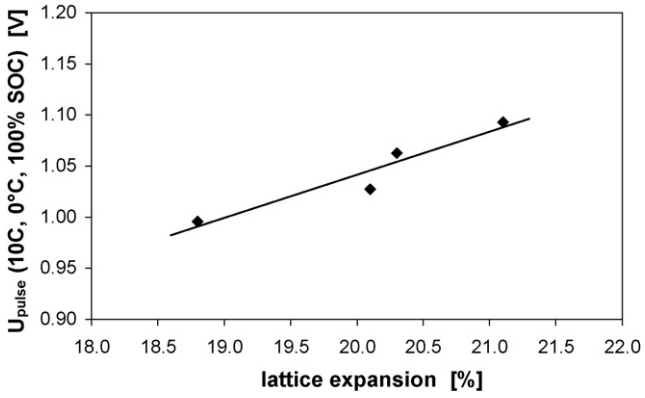

Fig. 6. Relationship between lattice expansion of hydrogen storage alloys caused by hydrogen intercalation and power performance of NiMH cells fabricated with these alloys.

Electrochemical reactions, but also corrosion reactions take profit from an increase of the surface area of the negative electrode and/or the reduction of the particle size as well. Therefore, effects associated with lattice expansion should result in an improvement of the power performance of the negative electrode, as long as the destructive effects associated with enhanced corrosion do not become overcompensating. Positive effects due to electrochemical grinding for this reason are expected at an early stage of cell life. At this stage, the difference in unit cell volume between hydride phase and unhydrided host structure could be a good measure for the mechanical stability of the alloy, as long as changes in mechanical properties, as elasticity or hardness, are neglected. Consequently, alloys with high-cracking rate should show better initial power performance (see Fig. 6).

However, variations of the composition of the hydrogen storage alloy do not only change the extent of lattice expansion during hydrogen intercalation, but also other properties of the alloy host structure and the hydride phase as well. Therefore, the relationship between power performance and surface area plus particle size at one hand, and the influence of the chemical composition with respect to micro-mechanical properties on the other hand, needs to be confirmed independently by experiments without changing the alloy composition. This can be done in two different ways. The pulverisation of the alloy proceeds with the number of electrochemical charge and discharge cycles. This phenomenon has been described already in detail [3,29] and is known as electrochemical grinding. Consequently, cells exposed to a high number of electrochemical cycles show a higher amount

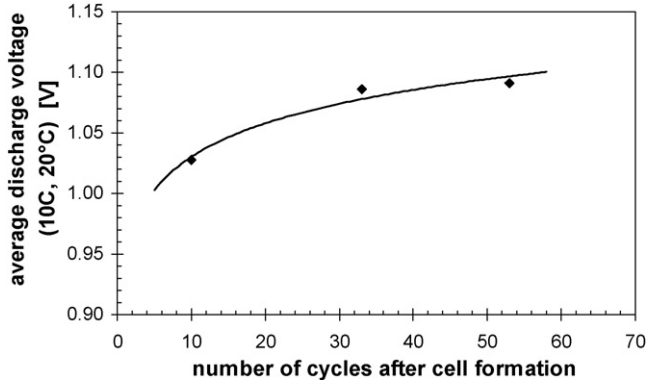

Fig. 7. Power performance of NiMH cells vs. number of initial activation cycles.

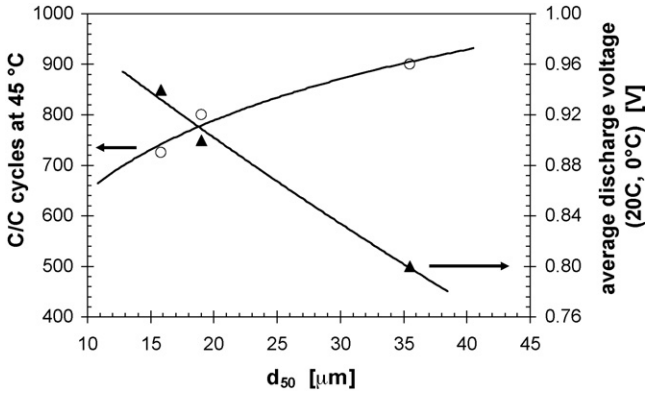

Fig. 8. Power performance and cycle life of hydrogen storage alloys comprising identical chemical composition but different particle size ((▲) power performance, discharge at 0 °C at 20*C* rate; (◯) cycle life at 45 °C).

of pulverisation of the alloy, compared to cells exposed to only few electrochemical cycles [30,31]. As is shown in Fig. 7, cells with a higher number of charge/discharge cycles show a significantly better power performance at an initial state of life, indicated by a higher average discharge voltage during a discharge with 10*C* rate at 20 °C. The improvement with respect to power performance is mostly significant within the first few cycles after cell formation. A higher number of activation cycles results in a minor increase of the power performance, as is indicated by a higher average discharge voltage during a high-rate discharge.

The importance of the influence of particle size of the hydrogen storage alloy on the power performance, could be further confirmed by a series of experiments using hydrogen storage alloy powders with the same chemical composition but different particle sizes. This allows for the separation of the particle size effect from the effect of the chemical composition. The d_{50} value from a particle size distribution measurement was used as a measure for the particle size. The power performance of NiMH cells employing hydrogen storage alloy powders with different particle sizes increases as the particle size of the alloy decreases (see Fig. 8). However, as the particle size decreases, the cycling stability of the alloy decreases (also shown in Fig. 8). The conflicting behaviour between cycle life and power performance will be discussed in some more detail in the following section.

3.2. Cycle life of NiMH cells

Cycle and calendar life of NiMH cells has been already studied in detail [32–36], because the improvement of cycle life has been the focus of hydrogen storage alloy development for many years. It is still an ongoing subject of research in the field of NiMH batteries. Especially, the influence of the alloy composition has been studied intensively [3,37–40]. In the past years more and more attention was paid to clarifying the fundamental principles, which are limiting the cycle life of NiMH batteries [41–44]. As a summary of the work published so far it is clear, that the negative electrode and especially the hydrogen storage alloy plays the dominant role for the cycle life of NiMH batteries. The life limiting mechanisms in NiMH cells are related to the corrosion of the alloy active material to a large extend. The corrosion reaction is given in (5) in a simplified form, disregarding the exact chemical composition of the alloy:

$$2M + H_2O \rightarrow MH + MOH \quad (5)$$

The consumption of water and the production of hydrogen, are both effects related to the alloy corrosion. They can become as severe as is the loss of active alloy material, and may therefore be life limiting. The reason for this becomes more clear, when cell layout and balancing details are taken into account. Usually, excess alloy is used in sealed NiMH cells. Therefore, the capacity of these cells is limited by the positive electrode. When these NiMH cells are exposed to a full charge, oxygen starts to evolve at the positive electrode, which can be consumed very rapidly at the negative electrode. Also hydrogen gas can be produced at the negative electrode during charge at high rates and/or low temperatures as a side reaction. For this reason, a pressure increase is observed during overcharge of NiMH cells. It is moderate, if low to medium currents are used, because hydrogen can easily be absorbed by the excess alloy. However, during corrosion, the amount of the negative excess capacity decreases due to a reduction of the alloy content and the absorption of hydrogen produced by the corrosion reaction as well. This leads to a misbalancing of the cell. As soon as negative excess capacity is exhausted, hydrogen starts to evolve during charging of the cell, which cannot be absorbed by the alloy anymore, due to lacking excess capacity. In this case a significant increase of the cell pressure during a full charge is observed and venting may be the consequence. The consumption of water, due to alloy corrosion leads to a concentration of the alkaline electrolyte and finally to a drying out of the cell. As a consequence electrochemical electrode potentials shift to different values and the impedance of the cell increases, as is shown in Fig. 9.

In case of AB_5 alloys using at the A-side mischmetal (Lm) rather than pure lanthanum and at the B-side a multielement composition rather than pure nickel, the corrosion processes lead to a change in the chemical composition of the alloy. Rare earth elements are found to form deposits of rare earth hydroxides at the surface of the alloy particles. For alloys of the type

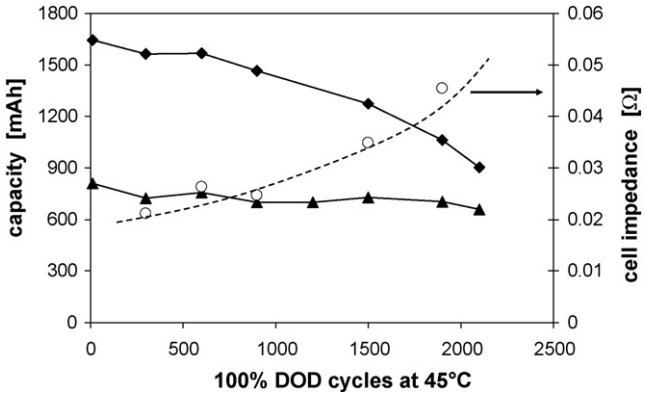

Fig. 9. Cycle life behaviour of NiMH cells at 45 °C (100% DOD) with respect to capacity of the negative and positive electrode and the cell impedance as well ((♦) capacity of the negative electrode; (▲) capacity of the positive electrode; (◯) cell impedance).

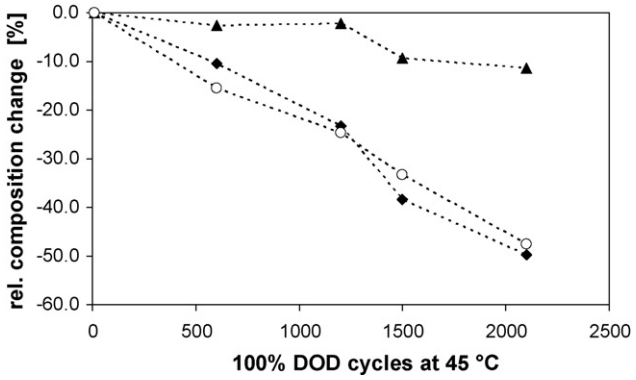

Fig. 10. Relative change in alloy composition during cycling at 45 °C, charge/discharge at *C* rate, 100% DOD ((♦) Al; (◯) Mn; (▲) La).

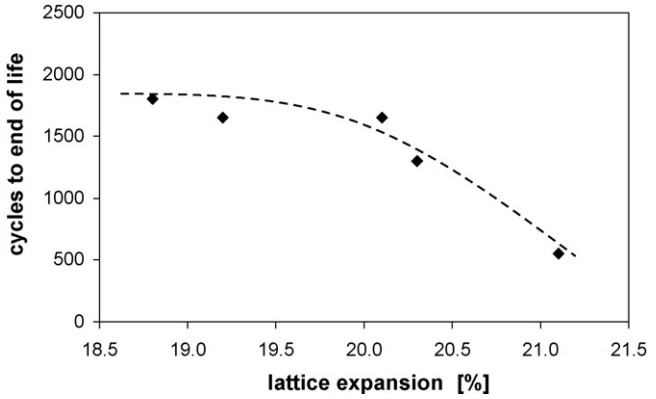

Fig. 12. Relationship between lattice expansion during hydrogen intercalation and cycle life of hydrogen storage alloys for NiMH batteries.

$Lm(Ni,Co,Al,Mn)_5$ especially, aluminium and manganese dissolve in the alkaline electrolyte and are found to be deposited at the positive electrode. The loss of manganese and aluminium due to corrosion at the end of life can be as high as 40–50% with respect to the initial values (see Fig. 10).

The corrosion behaviour of hydrogen storage alloys depends on the chemical composition of the alloy, its physical properties (hardness, elasticity) and the cycling and storage conditions of the NiMH cell (temperature, cycle profile, etc.) as well. The substitution of nickel with cobalt in AB_5 type alloys leads to a significant improvement of cycle life. Substitution of nickel with manganese however, results in a minor improvement in terms of cycle life. Furthermore cycle life tends to decrease, if the manganese content exceeds a certain value (see Fig. 11). The effect of cobalt with respect to the improvement of cycle life has several reasons. Srinivasan and co-workers [41] emphasised the importance of alloy integrity during cycling, which might be even more important with respect to cycle life, than the corrosion resistance of the alloy in alkaline electrolytes. Chartouni et al. [40] are ascribing the stabilising effect of cobalt mainly to the improvement of the mechanical properties of the alloy leading to a reduced tendency of cracking during consecutive hydrogen absorption and desorption. In summary, this results in a much lower pulverisation rate during consecutive electrochemical cycles for cobalt containing alloys.

The increase of the corrosion rate due to the pulverisation of the alloy is not only related to the increase of the surface area of the electrode, but also to an effect of instantaneous corrosion of the fresh alloy surface produced in the grain cracking process. Consequently, alloys with low-lattice expansion during hydrogen intercalation should show less tendency to pulverise, thus leading to reduced corrosion and therefore higher cycle life as shown in Fig. 12.

The cycling regime itself has an important impact on the cycle life behaviour of NiMH cells. As chemical or electrochemical reaction rates depend on temperature, an increase of the temperature leads to an enhanced corrosion rate. The amount of hydrogen intercalated or de-intercalated during electrochemical cycling is determined by the depth of discharge (DOD) in the specific cycling profile. The decrepitation rate of the alloy therefore is more pronounced for high DODs, due to a higher lattice expansion and contraction.

Leblanc et al. [44] confirmed that all aluminium, which was dissolved from the bulk alloy, was quantitatively deposited at the positive electrode. They concluded that the aluminium content of the positive electrode may serve as a direct indicator for the corrosion rate of Al-containing hydrogen storage alloys. In case of 100% DOD cycling, a nearly linear relationship was found for the corrosion rate and the cycle number (see Fig. 13). The slope

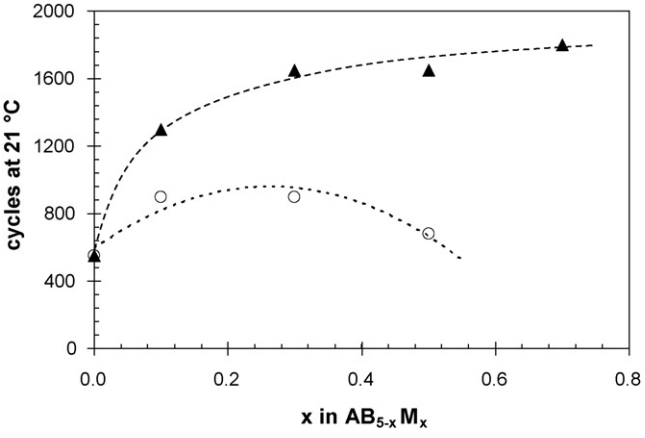

Fig. 11. Cycle life of alloys with different chemical composition ((◯) Mn; (▲) Co).

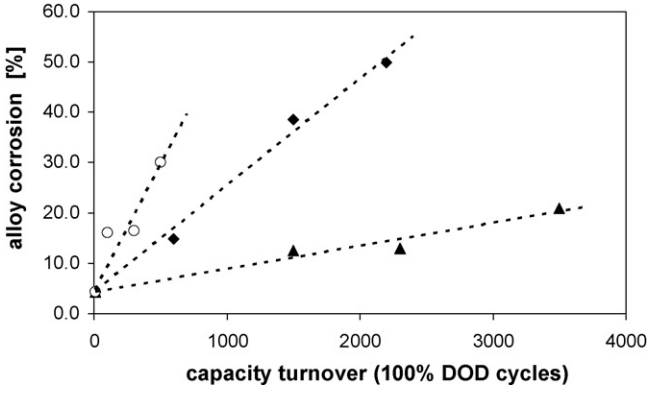

Fig. 13. Amount of corroded alloy as a function of cycle number and temperature during *C*/*C* cycling, 100% DOD ((▲) 23 °C; (♦) 45 °C; (◯) 60 °C).

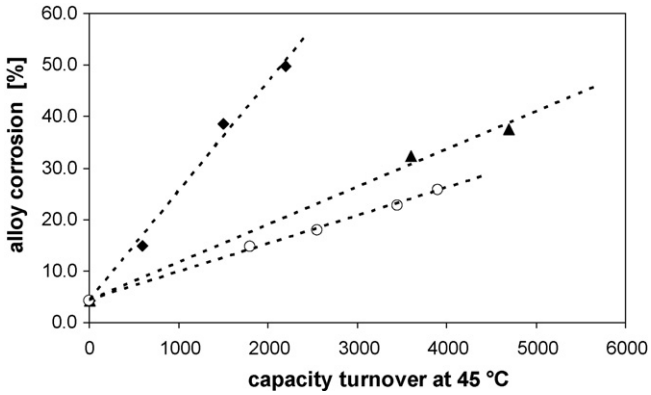

Fig. 14. Amount of corroded alloy as a function of cycle number and DOD, *C*/*C* cycles at 45 °C ((♦) 100% DOD; (▲) 50% DOD; (◯) 20% DOD).

increases with increasing temperature. From this temperature behaviour an activation energy of 54 kJ mol^{-1} can be calculated for a alloy consisting of mischmetal, nickel, cobalt, aluminium and manganese.

A linear behaviour was also found between cycle number and corrosion rate for different DODs. The alloy corrosion seems to increase exponentially with increasing DOD (see Fig. 14).

4. Conclusion

Due to their performance and robustness, NiMH batteries have been established in the HEV-market. Especially for this application, high-power performance and high cycle and calendar life are key issues. Besides that high-charge acceptance at high temperature and low-self-discharge are required. For power and life performance, the hydrogen storage alloy plays a dominant role and is therefore still a field of intensive development work. In our work we were able to show, that power performance and cycle life behaviour are connected to each other mainly by the electrochemical properties of the hydrogen storing alloy and often via a reciprocal relationship. In most cases changes in alloy composition or morphology improving power performance lead to inferior life and vice versa. In terms of power performance at medium- and high-discharge rates, the hydrogen storage alloy was found to be crucial for the temperature dependency of the cell. The rate limitation at medium-current rates in the range from 1*C* rate to 10*C* rate was found to be present in the short-term behaviour of the negative electrode, most probably related to charge transfer phenomena. At higher rates, diffusion limitations were found to be present at both electrodes. But they are more pronounced at the negative electrode. Charge transfer resistance and diffusion resistance as well depend on the surface area of the electrode and the particle size. However, as soon as hydrogen storing alloys are getting in contact with alkaline electrolytes, corrosion of the alloy starts, thus leading to the formation of surface films and a change of the chemical composition in the boundary zone, near to the surface of the alloy particles. The corrosion rate also depends on the electrochemically active surface area, as power capability with respect to discharge rate does. Hydrogen intercalation and de-intercalation is correlated to the lattice expansion and contraction as a consequence of different unit cell volumes of the host alloy and the hydride phase. Consequently, consecutive electrochemical cycles produce mechanical stress to the alloy particles with cracking as the final consequence. In summary, stability against corrosion and pulverisation on one hand and good electrochemical performance on the other hand side, both strongly depend on the chemical composition of the alloy, its morphological properties and the applied cycling regime. Therefore, the chemical composition and the morphology of the hydrogen storage alloy has to be designed for the special application, with respect to electrochemical, structural and micro-mechanical properties. The appropriate selection of the alloy with regard to the specific application is a key issue for guaranteeing good all-over performance of the cells in a NiMH-battery over a long period of time.

Acknowledgements

Support for research and development of materials for nickel–metal hydride cells and batteries at VARTA by the Commission of the European Union (CEU) is highly appreciated. The authors thank their numerous colleagues not named individually for their valuable contributions.

References

[1] C.D.S. Tuck (Ed.), Modern Battery Technology, Ellis Horwood, New York, 1991.
[2] D. Berndt, Maintenance Free Batteries, Research Studies Press, Taunton (England), 1997.
[3] J.J.G. Willems, Philips J. Res. 39 (Suppl. 1) (1984).
[4] H. Ogawa, M. Koma, H. Kawano, J. Matsumoto, J. Power Sources 12 (1988) 339.
[5] F. Meli, L. Schlapbach, J. Less Common Met. 172 (1991) 1252.
[6] F. Lichtenberg, U. Köhler, A. Fölzer, N.J.E. Adkins, A. Züttel, J. Alloys Compd. 2253–2254 (1997) 570.
[7] FreedomCar Test Manual for Power-assist Hybrid Electric Vehicles, version, October 2003.
[8] C. Iwakura, K. Fukuada, H. Senoh, H. Inoue, M. Masuoka, Y. Yamamoto, Electrochim. Acta 43 (1998) 2041.
[9] H. Ye, Y.X. Huang, T.S. Hung, H. Zhang, J. Alloys Compd. 330–332 (2002) 886.
[10] H.B. Yang, T. Sakai, T. Iwaki, S. Tanase, H. Fukumaya, J. Electrochem. Soc. 150 (2003) A1684.
[11] M.S. Wu, H.R. Wu, Y.Y. Wang, C.C. Wan, J. Appl. Electrochem. 33 (2003) 619.
[12] H. Ye, B. Xia, W. Wu, K. Du, H. Zhang, J. Power Sources 111 (2002) 145.
[13] H. Pan, J. Ma, C. Wang, C.P. Chen, Q.D. Wang, Electrochim. Acta 44 (1999) 3977.
[14] H.H. Uchida, Y. Watanabe, Y. Matsumura, H. Uchida, J. Alloys Compd. 231 (1995) 679.
[15] W. Chen, Z. Tang, H. Guo, Z. Liu, C. Chen, Q. Wang, J. Power Sources 74 (1998) 34.
[16] F. Liu, S. Suda, J. Alloys Compd. 232 (1996) 204.
[17] M. Enyo, Electrochim. Acta 11 (1994) 1715.
[18] T. Maoka, M. Enyo, Electrochim. Acta 26 (1981) 607.
[19] J.H. Chun, K.H. Ra, N.Y. Kim, J. Electrochem. Soc. 149 (2002) E325.
[20] C. Iwakura, M. Matsuoka, T. Kohno, J. Electrochem. Soc. 141 (1994) 2306.
[21] C. Iwakura, M. Miyamoto, H. Inoue, M. Matsuoka, Y. Fukumoto, J. Alloys Compd. 231 (1995) 558.
[22] H. Ye, H. Zhang, J. Electrochem. Soc. 149 (2002) A122.
[23] X. Yuan, N. Xu, J. Electrochem. Soc. 149 (2002) A407.
[24] P. Arora, R.E. White, M. Doyle, J. Electrochem. Soc. 145 (1998) 3647.

[25] R. Spotnitz, J. Power Sources 113 (2003) 72.
[26] J. Shim, R. Kostecki, T. Richardson, X. Song, K.A. Striebel, J. Power Sources 112 (2002) 222.
[27] D.P. Abraham, J. Liu, C.H. Chen, Y.E. Hyung, M. Stoll, N. Elsen, S. MacLaren, R. Twesten, R. Haasch, E. Sammann, I. Petrov, K. Amine, G. Henriksen, J. Power Sources 119 (2003) 511.
[28] J. Klepris, G. Wójcik, A. Czerwinski, J. Skowronski, M. Kopczyk, M. Beltowska-Brzezinska, J. Solid State Electrochem. 5 (2001) 229.
[29] P.H.L. Notten, R.E.F. Einerhand, J.L.C. Daams, J. Alloys Compd. 231 (1995) 604.
[30] M. Geng, J. Han, F. Feng, D.O. Northwood, J. Electrochem. Soc. 146 (1999) 2371.
[31] J. Han, F. Feng, M. Geng, R. Buxbaum, D.O. Northwood, J. Power Sources 80 (1999) 39.
[32] P. Bernard, J. Electrochem. Soc. 145 (1998) 456.
[33] L. Le Guenne, P. Bernard, J. Power Sources 105 (2002) 134.
[34] O. Arnaud, L. Le Guenne, C. Audry, P. Bernard, J. Electrochem. Soc. 152 (2005) A611.
[35] H. Kaiya, T. Ookawa, J. Alloys Compd. 231 (1995) 598.
[36] W. Zhang, A. Visintin, S. Srinivasan, A.J. Appleby, H.S. Lim, J. Power Sources 75 (1998) 84.
[37] G.D. Adzic, J.R. Johnson, S. Mukerjee, J. McBreen, J.J. Reilly, Electrochem. Soc. Proc.'97, vol. 16, 1997, p. 288.
[38] J.J. Reilly, G.D. Adzic, J.R. Johnson, T. Vogt, S. Mukerjee, J. McBreen, J. Alloys Compd. 293 (1999) 569.
[39] A. Merzouki, C. Cachet-Vivier, V. Vivier, J.Y. Nédélec, L.T. Yu, N. Haddaoui, J.M. Joulert, A. Percheron-Guegan, J. Power Sources 109 (2002) 281.
[40] D. Chartouni, F. Meli, A. Züttel, K. Gross, L. Schlapbach, J. Alloys Compd. 241 (1996) 160.
[41] C.S. Wang, M. Marrero-Cruz, J.H. Baricuatro, M.P. Soriaga, D. Serafini, S. Srinivasan, J. Appl. Electrochem. 33 (2003) 325.
[42] K. Shinyama, Y. Magari, K. Kumagae, H. Nakamura, T. Nohma, M. Takee, K. Ishiwa, J. Power Sources 141 (2005) 193.
[43] K. Shinyama, Y. Magari, H. Akita, K. Kumagae, H. Nakamura, S. Matsuta, T. Nohma, M. Takee, K. Ishiwa, J. Power Sources 143 (2005) 265.
[44] P. Leblanc, C. Jordy, B. Knosp, P. Blanchard, J. Electrochem. Soc. 145 (1998) 860.